Acceptance Simulations Studies for the Hall A High Resolution Spectrometers

A. Deur. LPC-Université Blaise Pascal. Deurpam@jlab.org.

November 21, 2000

Contents

Note. It is convenient to print this note in color in order to distinguish the data in the different figures.

1 Introduction

An accurate simulation of the High Resolution Spectrometer acceptance is needed to correct experimental data for acceptance effects or to compute the solid angle of the spectrometer. So far three different acceptances are available:

1. The first was made by H. Fonvieille and S. Jaminion for the VCS experiment (E93050).
2. The second was made by J.J. leRose.

3. The third was made by X. Jiang for the GDH experiment (E94010).

In this note we summarise the studies done on these three acceptance functions. A comparison between the different acceptance functions was done as well as a comparison with experimental data.

These experimental data were taken during the inclusive GDH experiment. They are in the Deep Inelastic Scattering domain. The data were taken with three overlapping momenta. This kinematic is chosen because the dependency of $\delta p/p$ with the virtual photon energy is small. The settings are:

- $\theta_{scattering} = 15.5^o$ (scattering angle)
- E=4.225 GeV (incident electron energy)
- E_p=1.696, 1.767 or 1.838 GeV (scattered electron energy)

The experimental data are corrected for trigger efficiency.

Some comparison using elastic ^{3}He(e,e')^{3}He experimental and simulated data will also be given.

2 Simulation

The three acceptance functions are used in different versions of a Monte Carlo. A manual explains where to find and how to use the Monte Carlo versions [1]. Four different versions exist for each HRS: one using the VCS acceptance, one using the GDH acceptance and two using J. leRose acceptance

2.1 The VCS Acceptance

The Monte Carlo using the VCS acceptance is called mce94010lpc.f. The ray tracing program Snake is used to generate particle tracks. The acceptance at the collimator place or magnet pole is fitted by a polynomial function. The VCS acceptance function is a logical function of the vector (θ_{target}, φ_{target}, $\delta p/p$, y_{target}). It says if the particle reaches the HRS focal plane according to the vector value. As a consequence only target quantities are available but no focal plane quantities. In addition the target quantities are the one generated by the Monte Carlo. They are not reconstructed from focal plane quantities.

2.2 J. leRose Acceptance

2.2.1 Transport and Inverse Functions

J. leRose used Snake as well (the difference is that J. LeRose uses a field model for the magnets while H. Fonvieille and S. Jaminion use the mapping). It is used to generate a transport function for each magnet element of the HRS. Collimator cuts are placed between the transport functions. Hence focal plan quantities are available in addition to the target quantities. The functions are inverted and used to reconstruct the target quantities using the focal plan quantities. A comparison between these quantities and the quantities generated at the target by the Monte Carlo shows very little differences (see Fig. 2 or the figures of the 15cm target study). These differences comes from the multiple scattering and the fact that the inversion of the transport functions is approximated. The small differences indicate also that we can use the VCS acceptance function even if the target quantities are not the reconstructed ones.

The Monte Carlo version using the J. leRose functions is called mce94010.f.

2.2.2 Transport Functions and Optics Database

Another Monte Carlo version exists. It uses the transport functions to go to the focal plan and then the experimental optics database to reconstruct the target quantities as ESPACE does. The advantage is that it follows the same procedure than ESPACE and it includes the imperfections of the experimental database. The database was optimised by M. Jones using the E94010 optic data taken during the experiment. The database version is db_full_had_31_elec_26. The Monte Carlo version is called mce94010r.f.

2.3 The GDH Acceptance

X. Jiang used Snake to reproduce the focal plane experimental data taken during the E94010 optics runs. The simulated spectra are stored in an ntuple and used as a weight. Hence no acceptance function exists and the Monte Carlo results depend on the statistic available in X. Jiang spectra. This is the main drawback of this version: The acceptance needs to be bin in four dimensions which ask for large statistics. So far the best compromise is a binning of ($\delta p/p$, θ_{target}, φ_{target}, y_{target}) of $8\times14\times20\times20$. However as long as no radiative corrections are folded in the data and if we have no $\delta p/p$, θ_{target} strong dependence of the acceptance then there is no correlation between the variables and we can use one dimensional spectra as a weight. The statistic is then not a problem anymore. This is the case for the inelastic experimental data:

- The dependence of the acceptance with θ_{target} is of second order.
- The radiative correction can be neglected since the $\delta p/p$ evolution with the photon virtual energy is flat: We can assume that the radiative processes make each $\delta p/p$ bin lose and gain the same amount of events.

Consequently the statistic will not be a problem for the comparisons in the deep inelastic domain. However It will be a drawback for the comparison using elastic data.

3 Comparisons of Target Quantities

We compare here the target quantities in the case of the deep inelastic runs. The only physics in the simulation is a Mott cross section. The comparisons between the simulations are absolute while the comparison with the experimental data is relative (we compare only the shape). However the elastic ^{3}He(e,e')^{3}He cross section analysis [2] shows that the absolute acceptance agreement is good to 5%.

All the figures shown are for the electron HRS.

3.1 40 cm Target

We present in figure 1 the relative momentum $\delta p/p$ in % for a 40 cm target length.

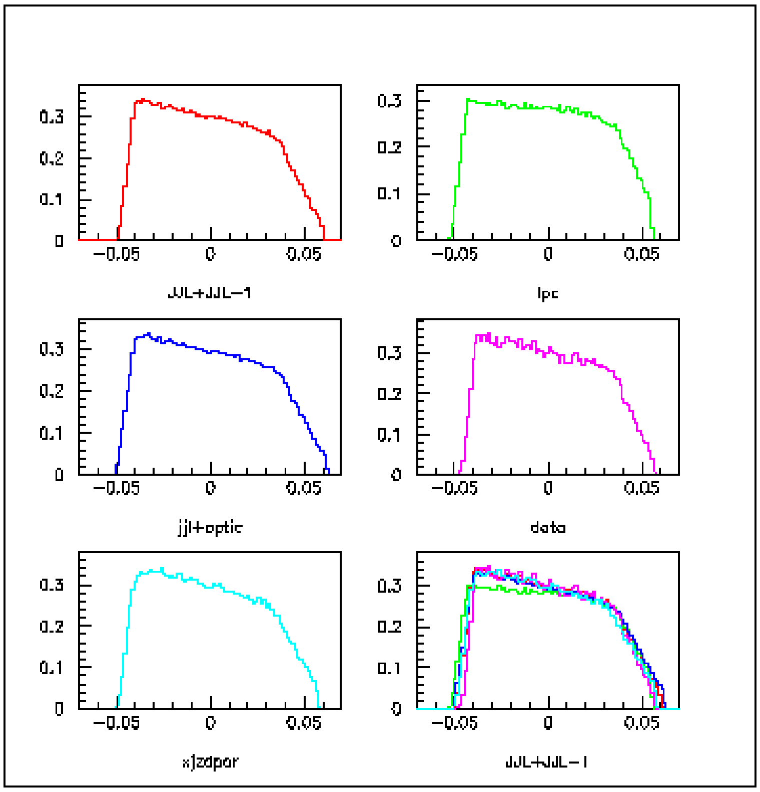

Fig. 1. Relative momentum $\delta p/p$ in % for a 40 cm target length. The top left plot is the simulation using J. leRose forward and inverse transport functions. The top right plot is the simulation using the VCS acceptance function. The middle left plot is the simulation using J. leRose forward transport functions and the experimental database. The middle right plot is the experimental data, the left bottom plot is the simulation using the GDH acceptance weight and the bottom right plot is the superposition of all the previous plots.

We see that the VCS function underestimates the acceptance for negative $\delta p/p$. All the acceptance simulations overestimate the acceptance range for negative $\delta p/p$. The VCS and GDH functions cut at the good range in positive $\delta p/p$ while the two using J. leRose functions overestimate the acceptance range.

The next figure presents θ_t, the vertical scattering angle at the target:

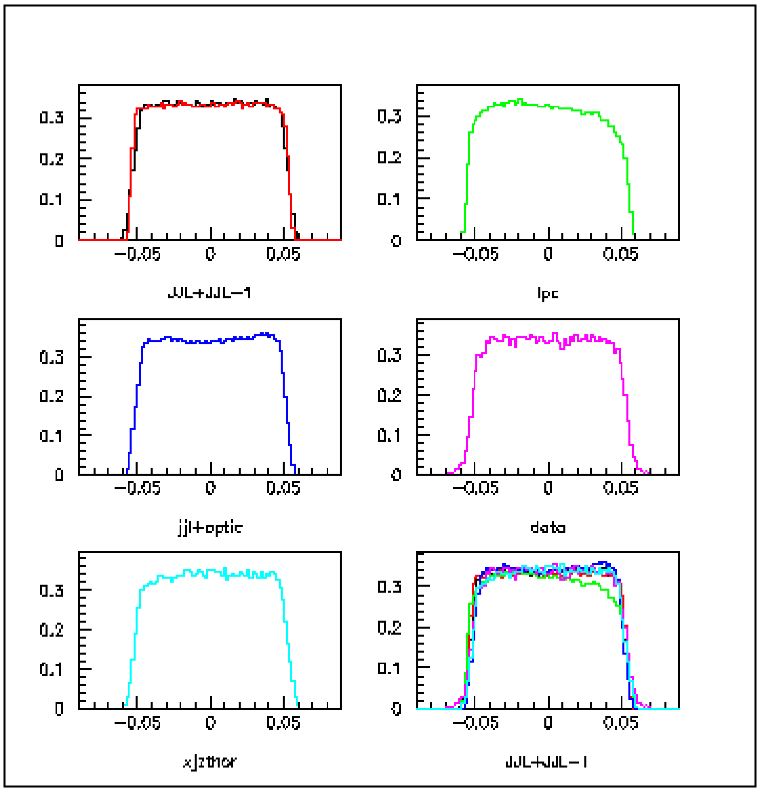

Fig. 2. The vertical scattering angle at the target θ_t for a 40 cm target length (in mr). On the top left plot, a first spectrum is the simulation using J. leRose forward and inverse transport functions (reconstructed angles) while a second spectrum is the angles generated at the beginning of the Monte Carlo. The differences between the two spectra come from the multiple scattering and the imperfection of the transport function inversion. The top right plot is the simulation using the VCS acceptance function. The middle left plot is the simulation using J. leRose forward transport functions and the experimental database. The middle right plot is the experimental data, the left bottom plot is the simulation using the GDH acceptance weight and the bottom right plot is the superposition of all the previous plots.

All the simulations are consistent and reproduce the data except the VCS acceptance function that underestimate the acceptance for positive θ_t.

In Fig. 3 we present φ_t the horizontal scattering angle at the target:

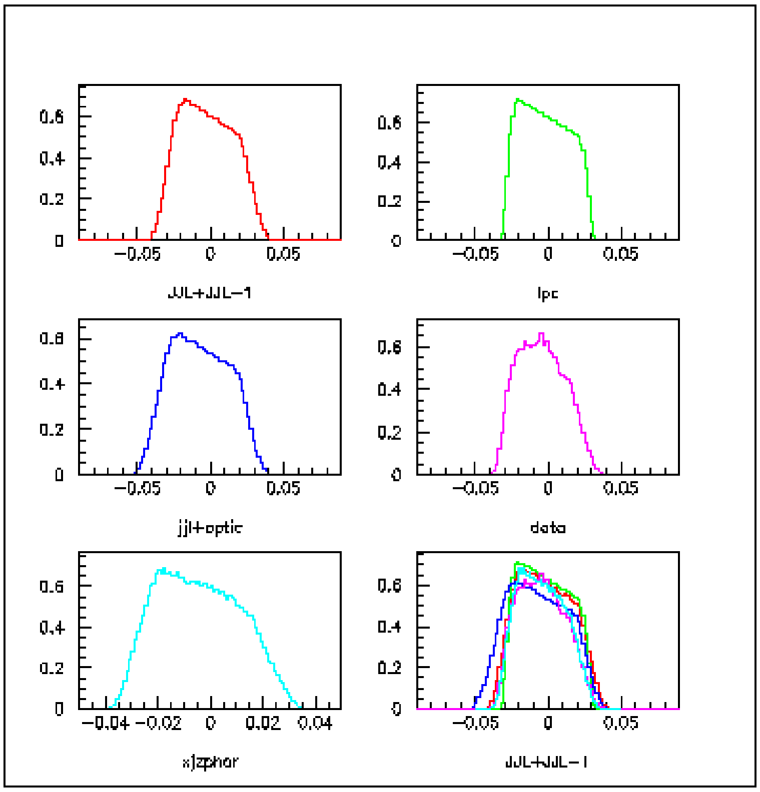

Fig.3. Horizontal scattering angle φ_t in mr for a 40 cm target length. The top left plot is the simulation using J. leRose forward and inverse transport functions. The top right plot is the simulation using the VCS acceptance function. The middle left plot is the simulation using J. leRose forward transport functions and the experimental database. The middle right plot is the experimental data, the left bottom plot is the simulation using the GDH acceptance weight (in a different scale than the other plots) and the bottom right plot is the superposition of all the previous plots.

The asymmetrical shape is due to the Born cross section variation within the angular acceptance. Without this dependence the shapes would be symmetric in respect to 0.

Both J. leRose and VCS acceptances overestimate the acceptance and the range for positive φ_t. The simulation using J. leRose forward functions to go at the focal plane and the experimental database to reconstruct fails to fit the acceptance. The GDH acceptance fits the data for positive φ_t.

All the simulations seem to overestimate the acceptance for positive φ_t. J. leRose and the GDH acceptances fit the acceptance range at negative φ_t while the VCS one is cutting a little too soon.

In Fig 4. we present y_t, the vertex horizontal position in the HRS frame:

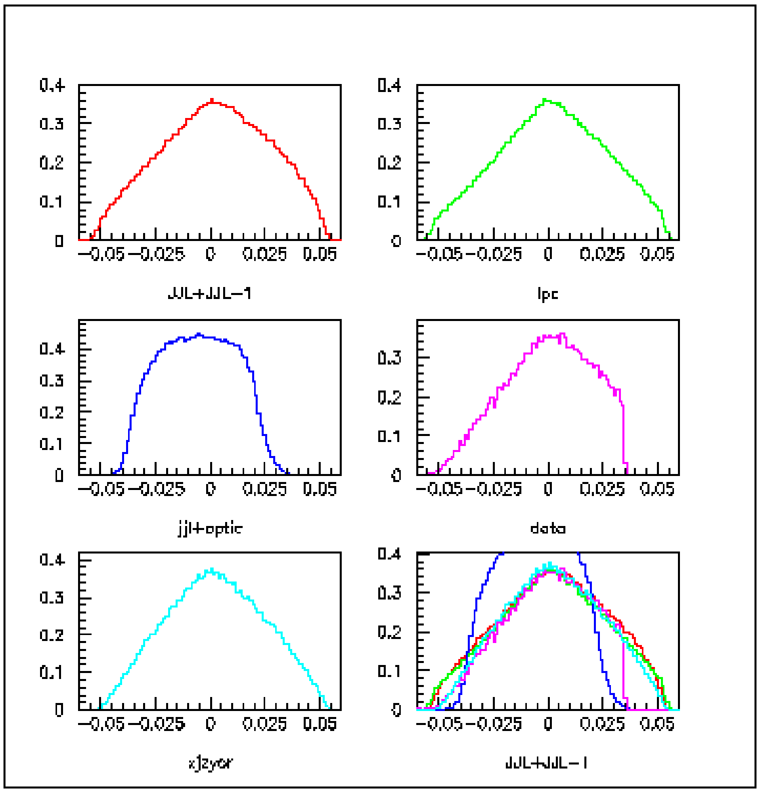

Fig. 4. The vertex horizontal position y_t for a 40 cm target length. The top left plot is the simulation using J. leRose forward and inverse transport functions. The top right plot is the simulation using the VCS acceptance function. The middle left plot is the simulation using J. leRose forward transport functions and the experimental database. The middle right plot is

the experimental data with a cut to remove the window contribution, the left bottom plot is the simulation using the GDH acceptance weight and the bottom right plot is the superposition of all the previous plots.

Again the simulation using J. leRose forward functions and the experimental database to reconstruct does not give a good y_t spectra.

As for φ_t, the y_t asymmetrical shape is all due to the Mott cross section. J. leRose and the VCS functions overestimate the acceptance for $y_t <$ -25 cm but agree together. It seems J. leRose functions overestimate the acceptance for positive y_t. The GDH acceptance fits well the data on the available range. The VCS acceptance gives a larger acceptance than the GDH one for positive y_t.

A discussion of these results will be given in section 5.

3.2 15 cm Target

Fig. 5 presents the relative momentum $\delta p/p$ in % for a 15 cm target length:

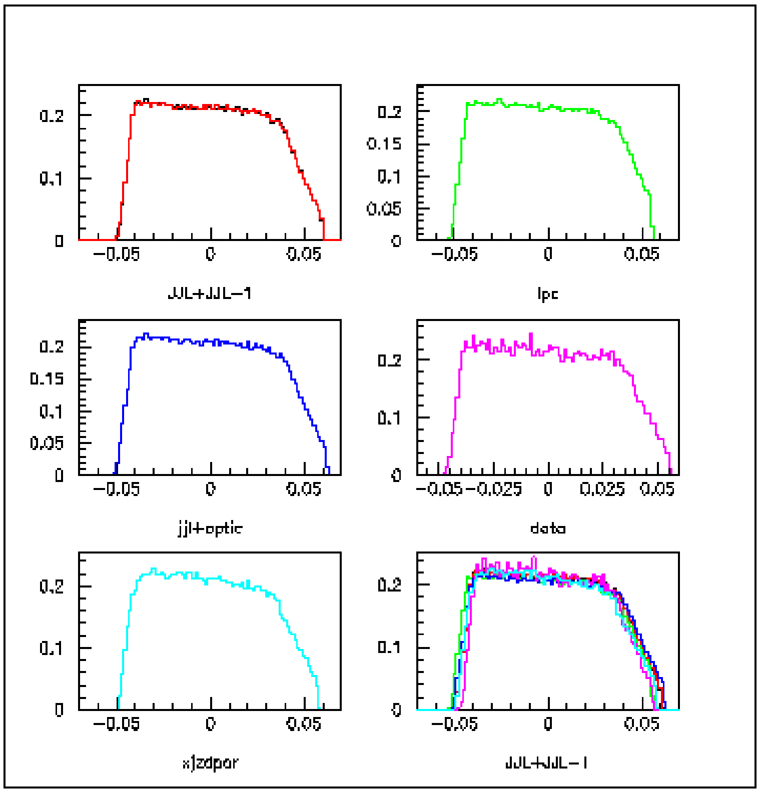

Fig. 5. Relative momentum $\delta p/p$ in % for a 15 cm target length. On the top left plot, a first spectrum is the simulation using J. leRose forward and inverse transport functions while a second spectrum is the $\delta p/p$ generated at the start of the Monte Carlo. The top right plot is the simulation using the VCS acceptance function. The middle left plot is the simulation using J. leRose forward transport functions and the experimental database. The middle right plot is the experimental data, the left bottom plot is the simulation using the GDH acceptance weight and the bottom right plot is the superposition of all the previous plots.

All the functions are consistent with the data. They all overestimate the negative $\delta p/p$ acceptance range and J. leRose functions overestimate the positive $\delta p/p$ acceptance range.

The figure 6. presents θ_t, the vertical scattering angle at the target:

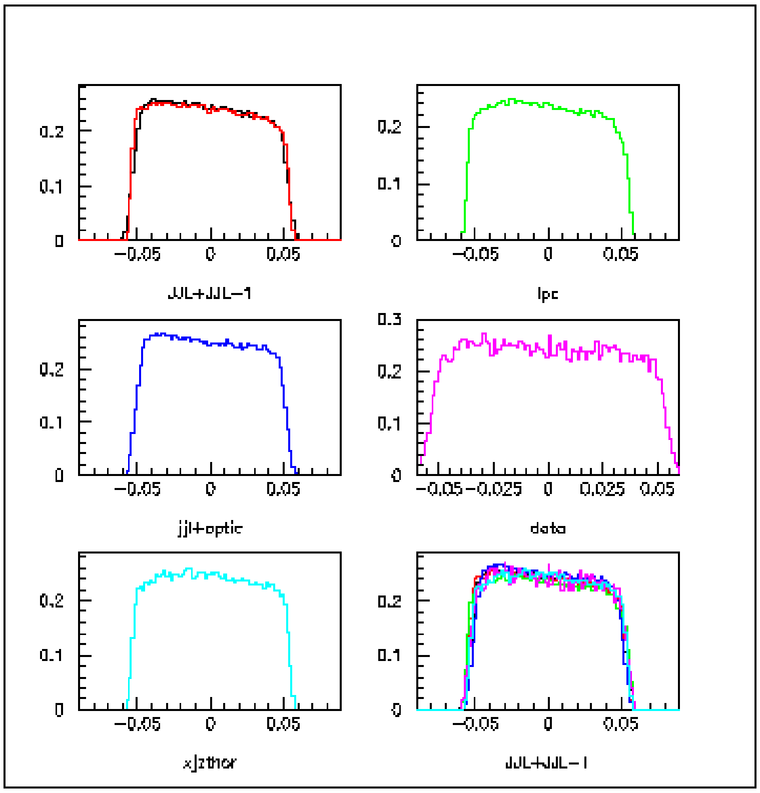

Fig 6. Vertical scattering angle θ_t in mr for a 15 cm target length. On the top left plot, a first spectrum is the simulation using J. leRose forward and inverse transport functions while a second spectrum is the angles generated at the start of the Monte Carlo. The top right plot is the simulation using the VCS acceptance function. The middle left plot is the simulation using J. leRose forward transport functions and the experimental database. The middle right plot is the experimental data, the left bottom plot is the simulation using the GDH acceptance weight and the bottom right plot is the superposition of all the previous plots.

All the simulations agree well with the experimental data.

Fig. 7. presents φ_t the horizontal scattering angle at the target:

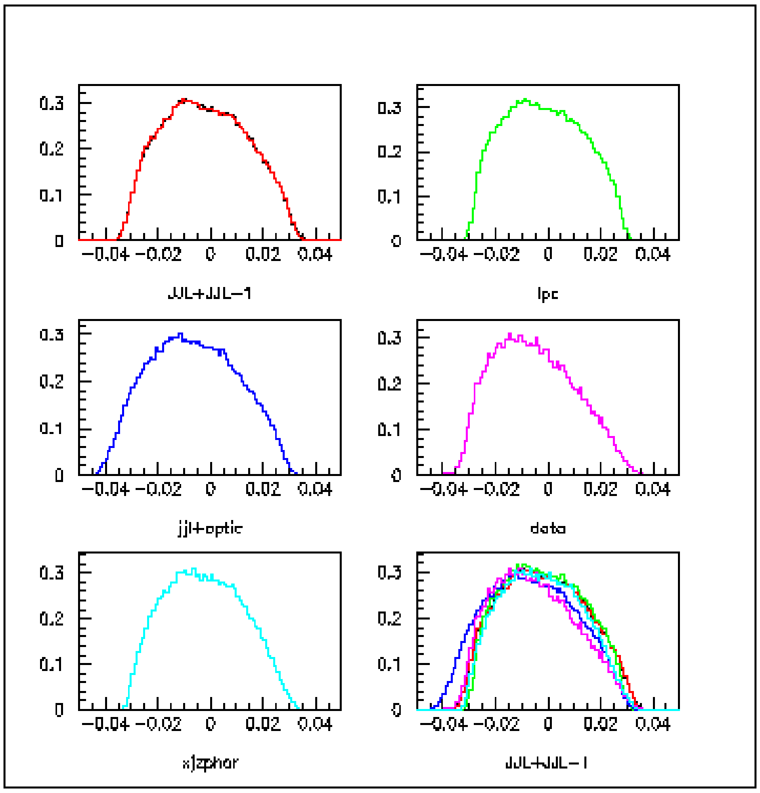

Fig. 7. Horizontal scattering angle φ_t in mr for a 15 cm target length. On the top left plot, a first spectrum is the simulation using J. leRose forward and inverse transport functions while a second spectrum is the angles generated at the start of the Monte Carlo. The top right plot is the simulation using the VCS acceptance function. The middle left plot is the simulation using J. leRose forward transport functions and the experimental database. The middle right plot is the experimental data, the left bottom plot is the simulation using the GDH acceptance weight and the bottom right plot is the superposition of all the previous plots.

We have the same conclusion than for the 40 cm Target: All the acceptance functions overestimate the acceptance for positive φ_t although the GDH function is closer to the data. The VCS and J. leRose functions also overestimate the acceptance range. Again the simulation using J. leRose forward functions and the experimental database to reconstruct fails.

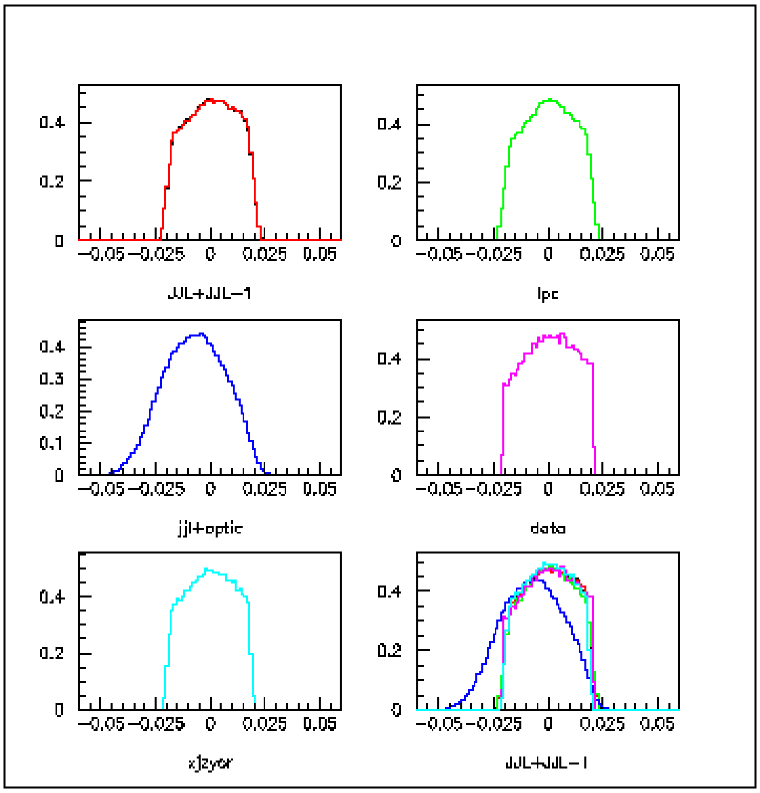

Fig 8. The vertex horizontal position y_t for a 40 cm target length. The top left plot is the simulation using J. leRose forward and inverse transport functions. On the top left plot, a first spectrum is the simulation using J. leRose forward and inverse transport functions while a second spectrum is the angles generated at the start of the Monte Carlo. The middle left plot is the simulation using J. leRose forward transport functions and the experimental database. The middle right plot is the experimental data with a cut to remove the window contribution, the left bottom plot is the simulation using the GDH acceptance weight and the bottom right plot is the superposition of all the previous plots.

All the simulations are in good agreement with the data but for the simulation using J. leRose forward functions and the experimental database.

3.3 1 cm target

All the simulations but the one using J. leRose forward functions and the experimental database are in good agreement with the data. I show the $\delta p/p$ results since it will be useful to understand the shape of the $\delta p/p$ spectra and why the VCS acceptance fails at 40 cm.

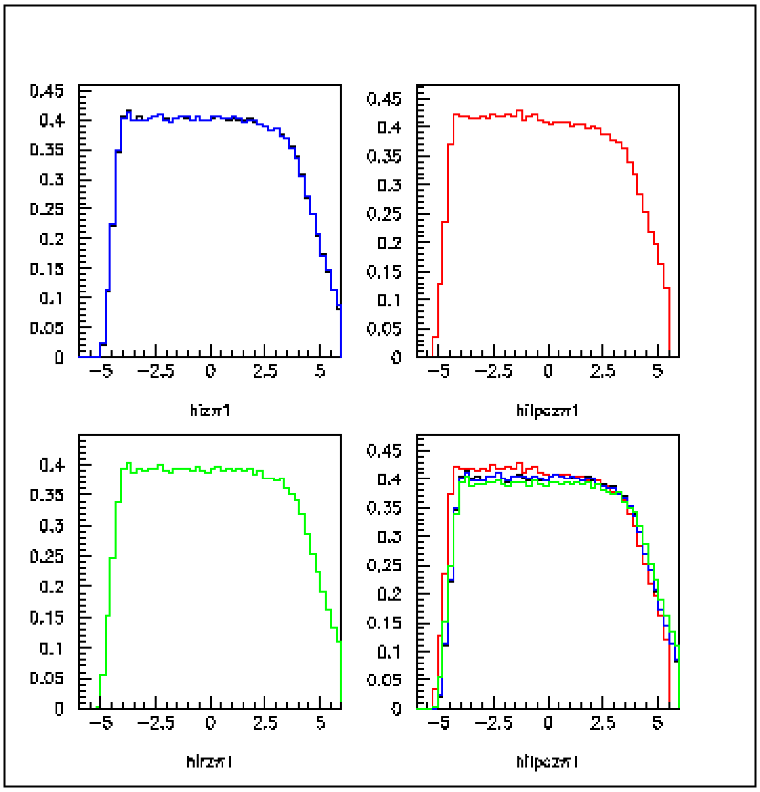

Fig. 9. Relative momentum $\delta p/p$ in % for a 40 cm target length. On the top left plot, a first spectrum is the simulation using J. leRose forward and inverse transport functions while a second spectrum is the $\delta p/p$ generated at the start of the Monte Carl. The top right plot is the simulation using the VCS acceptance function. The bottom left plot is the simulation using J. leRose forward transport functions and the experimental database. The bottom right plot is the superposition of all the previous plots and the experimental data.

4 Overlapping Momenta

During the experiment E94010 three HRS momentum settings were chosen close enough to have large overlaps. The glass window is cut so the target length is about 30 cm. The yield can be seen in fig. 10:

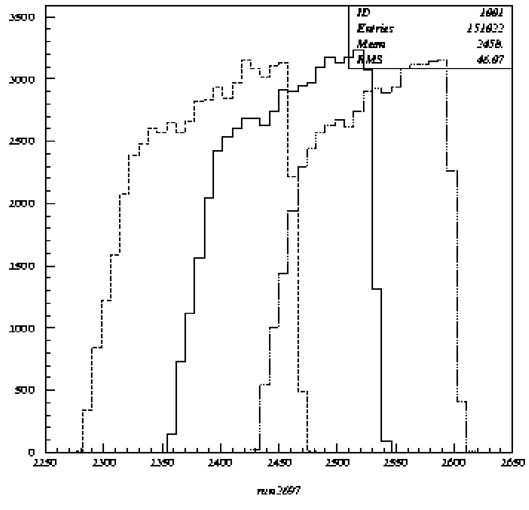

Fig. 10. The experimental yield taken in the Deep Inelastic Scattering domain for three close HRS momentum settings. The domain was chosen such as $\delta p/p$ variation with the virtual photon energy loss is small.

The $\delta p/p$ variation with the virtual photon energy loss is small so the spectra shape comes mostly from the HRS momentum acceptance. In the next two figures are plotted the experimental data corrected from the momentum acceptance. After correction the data trend must be flat and overlap the next momentum setting as long as the functions simulate well the data. In the figure 11 the correction is done using J. leRose acceptance functions. In the figure 12, the correction is done with the VCS acceptance function. The same study is not done with X. Jiang acceptance but must be close to the result obtained with J. leRose functions.

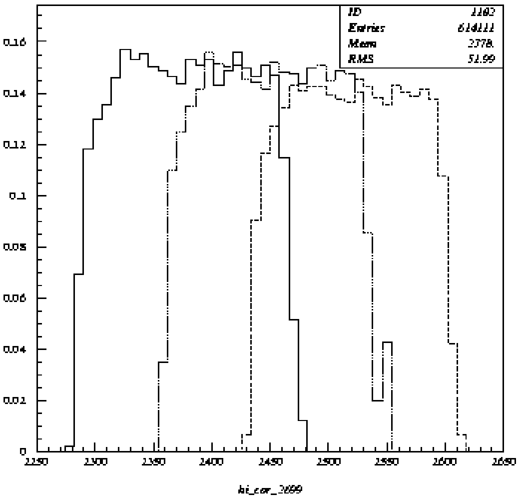

Fig. 11. The experimental yield corrected using J. leRose forward and inverse transport functions.

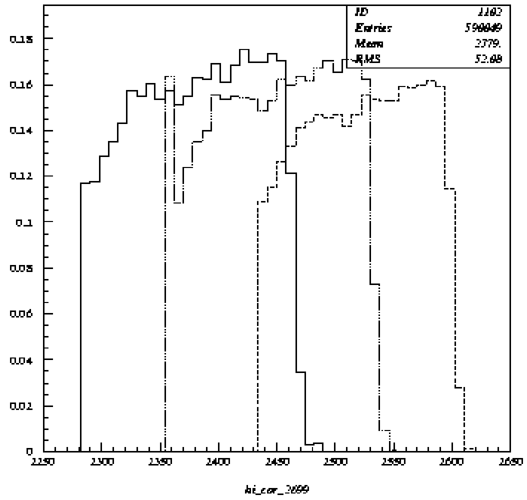

Fig. 12. The experimental yield corrected using the VCS acceptance function.

We can see in the fig. 11 that the spectra overlap nicely over the range $-3.5\% < \delta p/p < 2.7\%$. The slight oblique trend must be due to the $\delta p/p$ dependence with the virtual photon energy.

There is no such overlap in Fig. 12. This is due to the underestimate of the VCS acceptance in the negative $\delta p/p$.

5 Discussion

5.1 General Conclusions

- It appears that the Monte Carlo using J. leRose transport function and the optic database fails to reproduce the y_{target} and φ_{target} acceptances. The discrepancy may come from the fact that the simulated transport functions (let us call them JJL and let us call the inverse functions JJL^{-1}) may not reproduce exactly the true HRS transport functions (let us call them HRS and let us call the database HRS^{-1}). So the relation $JJL.JJL^{-1} \simeq 1$ is true while the relation $JJL.HRS^{-1} \simeq 1$ is not.

- X. Jiang function is better for 40 cm. There is a problem for all the simulation when trying to reproduce φ_{target}. The VCS acceptance function has a problem to reproduce $\delta p/p$ for long targets and forward angles.

- None of the acceptances give a good simulation of φ_{target} but this can come from the fact that a Mott cross section is not sufficient to reproduce the physics in this domain. This will be in investigated in the next part of this report when we compare experimental and simulated elastic data. In this case the physics is fully simulated.

5.2 $\delta p/p$ Acceptance

The VCS acceptance underestimate the negative $\delta p/p$ acceptance. The shape and why the VCS function fails can be understood by looking at the $\delta p/p$ spectra for 15 cm and 1 cm target:

For the 1cm target (fig. 9) the top of the $\delta p/p$ spectrum is almost flat. In the right side the acceptance begin to fall earlier than in the negative side. I we consider a 1 cm target as pointlike, the right side of the $\delta p/p$ spectrum correspond to particular couples (φ_t,θ_t).

With the 15 cm target (fig. 5) the top of the $\delta p/p$ spectrum has a slope. This slope increases as the target length increases (see fig. 1 for the 40 cm target). In this case we have a third degree of freedom, y_t, and to a couple (φ_t,θ_t) that makes the $\delta p/p$ acceptance to fall for 1 cm target can correspond to a $\delta p/p$ of the centre or the left side of the spectrum.

So the slope on the top of the $\delta p/p$ spectrum is the propagation of the positive $\delta p/p$ acceptance loss at 1 cm due to extended target effect. The VCS acceptance fails to reproduce the right slope for 40 cm target maybe because the cuts used to reproduce the right falling part of the acceptance are not good. We see in fig 2 that this discrepancy is accompanied by a discrepancy in positive θ_t. This indicates a too severe θ_t cut is done to reproduce the right part of the $\delta p/p$ acceptance.

5.3 φ_t and y_t Acceptance

The analysis done for the elastic data taken by the experiment E94010 shows that the discrepancy in the left side of y_t acceptance for a 40 cm target (see fig. 4) is due to a bad φ_t simulation. A cut on the positive values of φ_t (φ_t<10 mr) makes the simulated y_t shape to fit better the experimental data. This was studied with J. leRose acceptance simulation. See the note [2] for details.

6 Elastic Data

We rewrite here a study done in [2]. The study uses the experimental data with a 40 cm target, J. leRose transport functions and the GDH acceptance. We form the ratio between the experimental elastic cross section and the cross section simulations for cut values where the simulated acceptance fits well the data. The geometrical cuts (φ_t and θ_t) are extended, the ratio of the elastic simulated cross section over the experimental cross section is calculated for each new cut and plotted. The results are presented in fig. 13 and 14. We see a small cross section dependence with the φ_t cut size. The dependence is smaller with X. Jiang acceptance. A plateau is reached at large φ_t because we are going out of the HRS acceptance.

No strong dependence is seen with the θ_t cut size.

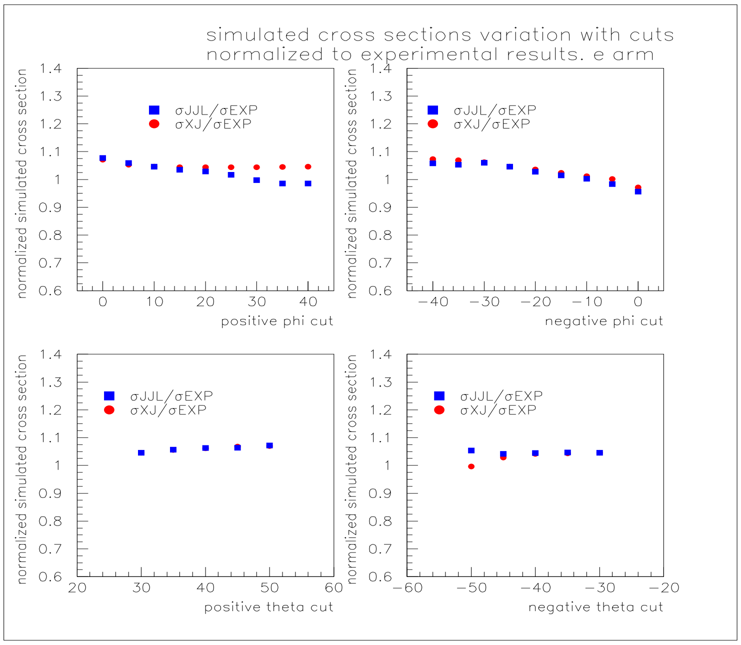

Fig. 13. Ratio of the elastic cross section simulated with the Electron Arm acceptance over the experimental cross section. It is calculated for different geometrical cuts. The squares are the cross sections simulated using J. leRose acceptance function divided by the experimental cross section. The circles are the cross sections simulated using X. Jiang acceptance simulation.

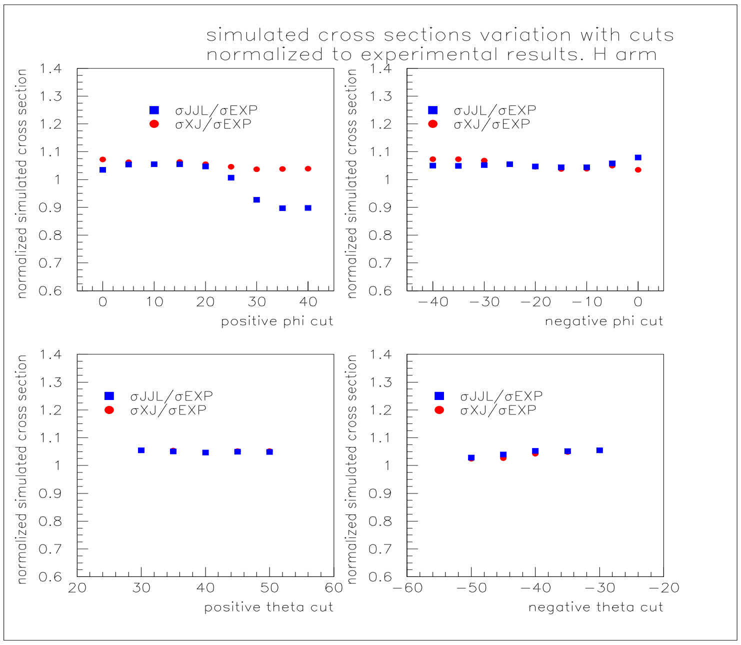

Fig. 14. Same than fig. 5 but for “Hadron” HRS.

The studies shows that the GDH acceptance is better suited for 40 cm targets. Reasonable cuts are:

- -25 $< \varphi_{target} <$ +15 mRd
- $\pm$30 $< \theta_{target} <$ $\pm$40 mRd
- -3.5 $< \delta p/p <$ +2.7 %

J. leRose transport functions give good result if we apply the following cuts:

- -25 $< \varphi_{target} <$ +10 mRd
- $\pm$30 $< \theta_{target} <$ $\pm$30 mRd
- -3.5 $< \delta p/p <$ +2.7 %

References

[1] A. Deur. Single Arm Monte Carlo for Polarised ^{3}He experiments in Hall A. Jefferson Lab Tech Note.

[2] A. Deur Elastic Cross Section Analysis for E94010. E94010 Technical Note.